FAR-INFRARED SPECTROSCOPIC IMAGES OF M83

G.J. Stacey[1], M.R. Swain[1], C.M. Bradford[1], M.J. Barlow[2], P. Cox[3], J. Fischer[4], S.D. Lord[5], M.L. Luhman[4], N.Q. Rieu[6], H.A. Smith[7], S.J. Unger[8], & M.G. Wolfire[9]

[1]Cornell University, Ithaca, NY, USA
[2]University College, London, UK
[3]Institute d'Astrophysique Spatiale, Paris,France
[4]Naval Research Laboratory, Washington D.C., USA
[5]IPAC, Cal. Inst. of Tech., Pasadena, CA, USA
[6]Observatoire de Paris-Meudon, France
[7]Harvard-Smithsonian Center for Astrophysics, Cambridge, USA
[8]Queen Mary and Westfield College, London, UK
[9]University of Maryland, College Park, MD, USA

ABSTRACT

We have mapped the nearby face on barred spiral galaxy, M83 in the bright [CII] 158 μm, [OI] 63 and 146 μm, [NII] 122 μm, and [OIII] 88 μm fine-structure lines with the Long Wavelength Spectrometer (LWS) on ISO. The maps are nearly fully sampled, and cover the inner $6.75' \times 6'$ region - essentially the entire optical disk. We also obtained a full LWS grating scan of the nucleus. The lines are detectable over the entire disk, and enhanced at the nucleus, where the [OI] 63 μm and [NII] lines are particularly strong. At the nucleus, the line ratios indicate a strong starburst headed by O9 stars. Surprisingly, the [OI] and [CII] line emission (from photodissociation regions) is not enhanced relative to [NII] (from low density HII regions) on the spiral arms. The line ratios are the same for the spiral arms and interarm regions. We find very strong emission in the [OIII] 88 μm, [OI] 146 μm, and [CII] lines at the intersection of the bar and spiral arm to the SW indicating particularly strong star formation activity there. The [OI] 63 μm/146 μm line ratio is quite small there likely the result of self absorption in the 63 μm line by enveloping clouds. The total luminosity of this emission peak is $\sim 1.2 \times 10^9 L_\odot$

Key words: galaxies: starburst – galaxies: individual: M83 – galaxies: ISM – infrared: galaxies

1. INTRODUCTION

The far-infrared (far-IR) fine structure lines that arise from abundant atoms and ions provide unique probes of the physical conditions of the interstellar medium in galaxies. Until ISO, most far-IR astronomical spectroscopy was performed using airborne, or balloonborne observatories. Unfortunately, the high background associated with these observatories prevented the detection of the far-IR lines from all but the brightest extragalactic sources. The cryogenic telescope on ISO dramatically changed this situation enabling for the first time detection of many of the lines from fairly large, systematically selected galaxy samples (e.g., Malhotra et al. 1997, Luhman et al. 1998). These studies demonstrate how the lines and far-IR continuum constrain the physical conditions of the ambient gas clouds, and the hardness and strength of the ambient interstellar radiation fields, thereby telling us much about the star formation history of these galaxies.

Galaxies are complicated beasts, and far-IR line emission can arise from a wide variety of regions - some currently forming stars, some not - within the galaxy. Therefore, to properly interpret spectra obtained from distant galaxies, it is important to examine as best we can the far-IR properties of various regions in nearby, resolved star forming galaxies. A fine example of such a galaxy is the nearby barred spiral galaxy M83. M83 has high surface brightness, is presented to us nearly face on ($i \sim 24°$) and has both well defined spiral arms and an optical bar that are resolvable at the spatial resolution of ISO's long wavelength spectrometer (LWS). At the distance of M83 ($d \sim 3.7$ Mpc), the 80 $''$ LWS beam subtends 1.5 kpc.

The highest priority project in the LWS Core Program 'The ISM in Normal Spiral Galaxies' was to map the brightest far-IR fine structure lines from M83. We used the LWS grating to map nearly the entire optical disk in the five brightest far-infrared fine structure lines: the [OI] (63 and 146 μm), [OIII] 88 μm, [NII] 122 μm, and [CII] 158 μm lines. The map is laid out on a rectangular 8×7 point grid that is nearly fully sampled ($45''$ step size), and covers nearly the entire optical disk. We also obtained a complete LWS grating scan (43 to 196 μm) at the nu-

Proceedings of the Conference "The Universe as seen by ISO". Paris, France, 20–23 October 1998 (ESA SP-427, March 1999)

cleus, and deeper, separate integrations for the [OIII] 52 μm and [NIII] 57 μm lines there. The total integration time for the project was $\sim$ 5 hours.

2. RESULTS AND DISCUSSION

2.1. Overall properties

The lines are all detected over much of the optical disk (Figures 1 to 5). The [CII], and [OI] 63 μm maps have particularly high signal to noise (S/N) ratios. The bright optical bar is apparent in each of the line maps, and the spiral arms are obvious in all but the lowest S/N [OIII] 88 μm and [OI] 146 μm maps. The integrated flux in all of the lines is $\sim 2.1 \times 10^8 L_\odot$, or $\sim$ 0.68% of the total far-IR flux from the galaxy ($L_{far-IR} \sim 3.1 \times 10^{10} L_\odot$). Over half of the line flux comes out in the bright [CII] 158 μm line, and 60% of the remaining flux comes out in the [OI] 63 μm line. These ratios are typical for spiral galaxies (cf. Stacey et al. 1991, Lord et al. 1996). For the discussion that follows, we will refer to several regions apparent in optical images of M83: the bright central nucleus, the bar extending about 2′ to the NE and SW of the nucleus, the spiral arms (especially the western arm prominent in Figures 3 and 5, and the intersection of this spiral arm and the southwestern bar.

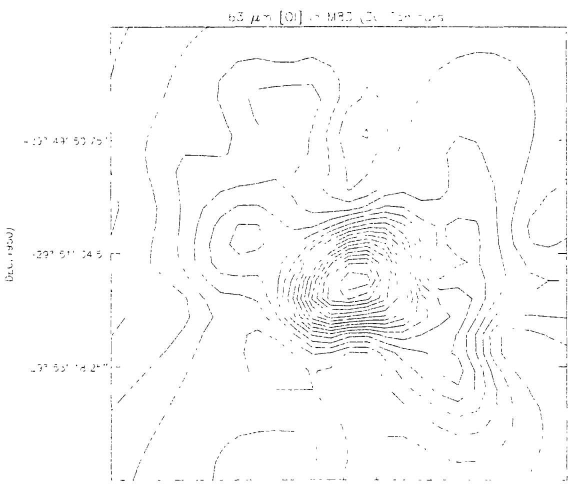

Figure 1. 63 μm [OI] map of M83. Contour intervals (1.5 σ) are 3.3% of the peak flux: 1.24 $\times 10^{-18}$ W cm^{-2} per 80″ beam.

2.2. Origins of the far-IR lines

It takes 14.5 and 35.1 eV photons to form N^+ and O^{++} respectively, so that the [NII], [NIII], and [OIII] line emission arises exclusively from ionized gas regions. Oxygen has nearly the same ionization potential as hydrogen (13.6 eV), so that the [OI] emission traces exclusively neutral gas clouds. However, since the ionization potential of carbon (11.4 eV) is

Figure 2. 88 μm [OIIII] map of M83. Contour intervals (1.5 σ) are 5% of the peak flux: 3.33 $\times 10^{-19}$ W cm^{-2} per 80″ beam.

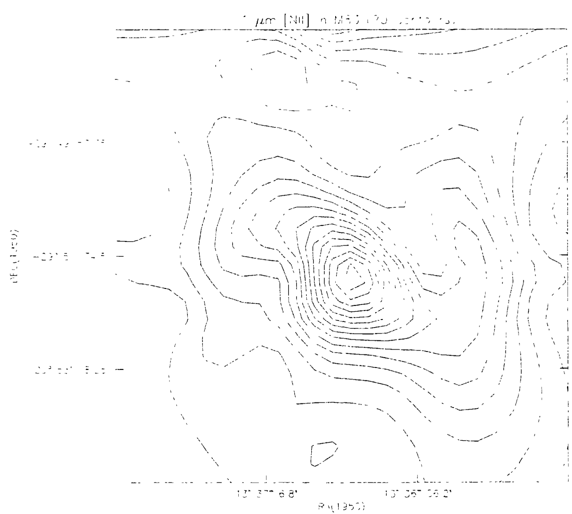

Figure 3. 122 μm [NII] map of M83. Contour intervals (2 σ) are 5% of the peak flux: 2.65 $\times 10^{-19}$ W cm^{-2} per 80″ beam.

less than that of hydrogen, C^+ is found both in ionized and neutral hydrogen gas regions. Furthermore, the [CII] emitting level has low excitation requirements so that the [CII] line is an important coolant for three major gas reservoirs (1) warm, dense, photodissociation regions (PDRs) on the surfaces of UV exposed molecular clouds (2) atomic clouds (T $\sim$ 100 K, n $\sim$ 30 cm^{-3}), and (3) extended, low density (ELD) HII regions (also know as the warm ionized medium, WIM). In galactic nuclei, it is clear that most of the observed [CII] emission arises from PDRs (Stacey et al. 1991). Integrated over the disks of normal spiral galaxies, however, [CII] likely arises from each component in roughly equal proportions (Madden et al. 1993, Geis et al. 1998). However,

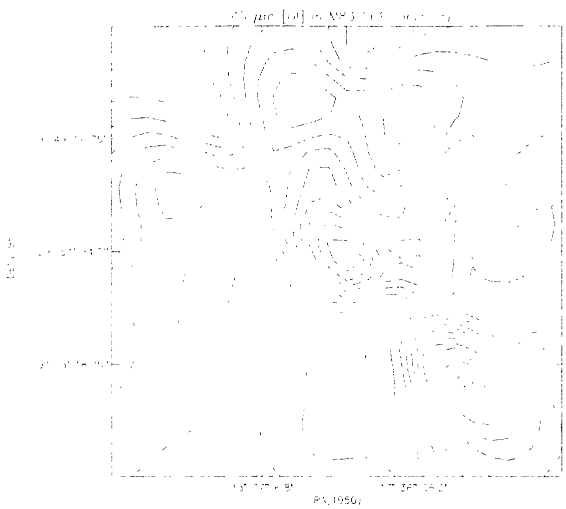

Figure 4. 146 μm [OI] map of M83. Contour intervals (1 σ) are 7.7% of the peak flux: 8.5 $\times 10^{-20}$ W cm^{-2} per 80″ beam.

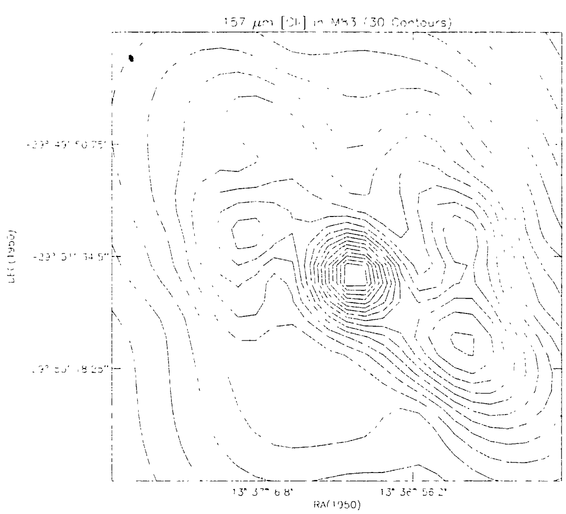

Figure 5. 158 μm [CII] map of M83. Contour intervals (3 σ) are 3.3% of the peak flux: 1.72 $\times 10^{-18}$ W cm^{-2} per 80″ beam.

it is possible to model the [CII] emission as arising from any of the three ISM components by modestly changing assumed cloud parameters, especially cloud density.

This situation can be ameliorated somewhat by comparing [NII] and [CII] emission. Since N^+ is only found in HII regions, and the critical density for the 122 μm line is similar to that of the 158 μm [CII] line in ionized gas regions, the [CII]/[NII] line ratio can be used to delineate the fraction of the observed [CII] emission that arises from the ELD/WIM subject only to an assumed N/C abundance ratio. We have made this calculation for the various regions of M83, and find that roughly 37% (nucleus), 30% (spiral arms), and 27% (interarm regions) of the observed [CII] emission arises from ELD/WIM HII regions in M83. Furthermore, the strength of the [OI] lines relative to [CII] indicates that little [CII] arises from 'atomic clouds'. Most of the remaining [CII] emission (that not arising from ELD/WIM) arises from the classic dense PDRs on molecular cloud surfaces.

2.3. The nucleus

The strongest line (and continuum) emission arises from the nuclear starburst region. The nucleus is especially prominent in the [OI] 63 μm, and [NII] 122 μm line emission for which the nuclear emission is twice as bright as any other region of the galaxy. The total line flux (dominated by the [CII] and [OI] 63 μm lines) is 1.8 $\times 10^7 L_\odot$ or $\sim 0.5\% L_{far-IR}$.

The complete LWS L01 spectrum reveals weak [OIII] 51.8 and [NIII] 57.4 μm line emission. The ratio of the [OIII] lines is insensitive to gas temperature, but gas density sensitive in the regime 100 $\leq n_e \leq 10^4$ cm^{-3}. For the nucleus, the line ratio, I[OIII] 52 μm/I[OIII] 88 μm ~ 1.05, so that $n_e \sim$ 250 cm $^{-3}$ - comparable to diffuse HII regions in M82 (Lord et al. 1996), but much larger than those in the Galaxy (ne ~ 3 cm^{-3}, Pettuchowski & Bennett 1993). The ratio of the [NIII] to [NII] lines is sensitive to the hardness of the ambient stellar UV radiation field. For the nucleus, I[NIII]/I[NII] ~ 0.9. This is much smaller than that for M82 (~ 2.1, Colbert et al. 1998) which means that the main sequence is headed by later type stars (Teff ~ 35,000 K, O9, (Rubin 1985) in M83 than for M82 (Teff ~ 37,000, O8). Assuming the same initial mass function (IMF), the starburst must be older in M83. If a single starburst occurred, it occurred about 10^7 years ago. Since the lines have similar excitation requirements, I[NIII]/I[OIII] is largely an N/O abundance indicator. For M83, I[NIII]/I[OIII]52 μm ~ 0.67 which means that N/O ~ 2.4 solar (Rubin 1985) - similar to the abundance ratios in the inner Galaxy (Lester et al. 1987). Enhanced N/O indicates more processing of the ISM.

The ratio of the two [OI] lines is sensitive to gas pressure. By factoring in the [CII] line emission that likely arises from PDRs we can decouple temperature and density. The observed line ratios are I[OI]63 μm/I[OI]146 μm ~ 17, and I[CII]/I[OI]63 μm~ 0.9. Using the PDR models of Wolfire, Tielens, and Hollenbach (WTH 1991) we find that the emitting clouds must be dense ($n_H \sim$ 3000 cm^{-3}), and exposed to high UV radiation fields, $G_o \sim 5000$ times the local interstellar radiation field. Surprisingly, the derived UV field is larger than that derived for M82: $G_o \sim 1000$ (Lord et al. 1996).

2.4. Spiral arms/interarm regions

The eastern and western spiral arms are discernible in all lines, but especially prominent in the (higher signal to noise ratio) [CII], [OI] 63 μm, and [NII] maps. The arm/interarm contrast is highest for the [OIII] 88 μm line suggesting that the earliest type stars reside in the spiral arms, consistent with their formation there. Somewhat unexpectedly, the [CII]/[NII]/[OI] line intensity ratios are roughly the same for the spiral arms and the interarm regions: there is no evidence for enhancement of PDR line emission on the spiral arms. This is surprising since one would expect relatively enhanced [OI] line emission on the spiral arms from the UV exposed molecular clouds in the arm star formation regions. Similarly, it is also surprising that the [CII] and [NII] line intensity ratio is the same on the spiral arms as it is in the interarm region. One might expect enhanced [CII] relative to [NII] due to spiral arm PDR emission. The star forming spiral arms are not distinguishable from the interarm regions by their line ratios. At the spatial resolution of ISO, the components of the ISM that give rise to the [OI], [NII], and [CII] lines must be well mixed. The [OI] line intensity ratio, I[OI] 63/I[OI] 146 μm is about 20 - consistent with rather high UV radiation fields ($G_o \sim 3000$, WTH). Subtracting off the ELD/WIM [CII] emission (30%), the [CII]/[OI] 63 μm ratio is 1.3 so that PDR models indicate rather dense clouds as well ($n_H \sim 3000$ cm^{-3}).

2.5. Bar/spiral arm interface

The bright NE-SW optical bar is apparent in the fine structure line maps. Particularly intriguing is that the [OI], [CII], and [OIII] lines are all strongly enhanced at the bar-spiral arm intersections (at $\sim$ 2' NE and SW of the nucleus), suggesting enhanced star formation activity in these regions. The [OI] 146 μm, [OIII], and [CII] lines are particularly strong at the SW bar-spiral arm interface (SW peaks in Figures 2, 4 and 5), where the lines are about as strong as they are at the nucleus! The far-IR continuum is $\sim$ 3 times weaker there so the line to continuum ratio is enhanced in this region: $\sim$ 0.7%. The I[OI] 63 μm/I[OI] 146 μm ratio is very small ($\sim 8 \pm 1.5$). Normally this suggests very strong UB radiation fields ($G_o \sim 10^5$), and very high gas densities ($n_H \sim 10^4$ cm^{-3}, WTH). However, the I[CII]/[OI] 63 ratio is unusually large ($\sim$ 1.3, subtracting off the [CII] emission from ELD/WIM), and if the UV fields and gas densities are as large as indicated, the line to continuum ratio should be small, $\leq 0.1\%$ - a factor of seven smaller than the observed ratio. The combined data are therefore inconsistent with any single component PDR model (WTH).

Optical depth effects in the 63 μm [OI] line may cause these unusual ratios. The 63 μm [OI] line has long been known to have appreciable optical depth (cf. Stacey et al. 1983, Stacey et al. 1993, Poglitsch et al. 1996), and ISO has shown that the [OI] line is often self absorbed towards massive, embedded star formation regions in the Galaxy (cf. Baluteau et al. 1998). The bright [OIII] emission at the SW bar-spiral arm intersection indicates a young massive star formation site there, so it is reasonable to expect the star clusters will still be embedded in their nascent molecular clouds. The [OI] 63 μm emission from these embedded star formation sites is then easily absorbed by neutral oxygen in the cooler blanketing clouds. The [CII] line is not affected by this mechanism since ionized carbon will not be found in these dark clouds, and the [OI] 145 μm line is not affected since it is a transition between excited states. If we assume that the self absorption has reduced the [OI] 63 μm line flux by a factor of 2.5 then a self consistent model can be made with ($G_o \sim 10^{3.3}$) and gas densities ($n_H \sim 10^4$ cm^{-3}, WTH). The SW bar region is strong in other indicators of star formation particularly in its Hα (de Vaucouleurs et al. 1983), and CO rotational line emission (e.g. Kenney & Lord 1991). Kenney & Lord (1991) have suggested that orbit crowding at the bar-spiral arm transition may have triggered a massive burst of star formation there. The bright far-IR fine structure line we observe there is consistent with this scenario.

REFERENCES

Baluteau, J.-P, et al. 1998, A&A 322, L33

Colbert, J.W., Malkan, M.A., Fischer, J., Lord, S., Luhman, M., Satyapal, S., Smith, H.A., Spinoglio, L., & Stacey, G.J. 1998, to appear in ApJ

Geis, N. et al. 1998 in prep.

Kenney, J.D.P., & Lord, S.D. 1991, ApJ 381, 118

Lester, D.F., Dinerstein, H.L., Werner, M.W., Watson, D.M., Genzel, R., & Storey, J.W.V. 1987, ApJ 320, 573

Lord, S.D., Hollenbach, D.J, Haas, M.R., Rubin, R.H, Colgan, S.W.J., & Erickson, E.F. 1996, ApJ 465, 703

Luhman, M.L., Satyapal, S., Fischer, J., Wolfire, M.A., Cox, P., Lord, S.D., Smith, H.A., Stacey, G.J., & Unger, S.J. 1998, ApJ 504, L11.

Madden, S.C., Geis, N., Genzel, R., Herrmann, F., Jackson, J.M., Poglitsch, A., Stacey, G.J., & Townes, C.H. 1993, ApJ 407, 579

Malhotra, S., Helou, G., Stacey, G.J., Hollenbach, D. Lord, S., Beichman, C.A., Dinerstein, H., Hunter, D.A., Lo, K.Y., Lu, N.Y., Rubin, R.H., Silbermann, N., Thronson, H.A. Jr., & Werner, M.W. 1997, ApJ 491, L27

Petuchowski, S.J. & Bennett, C.L. 1993, ApJ 405, 591

Poglitsch, A., Herrmann, F., Genzel, R., Madden, S.C., Nikola, T., Timmermann, R., Geis, N., & Stacey, G.J. 1996, ApJ 462, L43.

Rubin, R.H. 1985, ApJ S 57, 349

Stacey, G.J., Smyers, S.D., Kurtz, N.T., & Harwit, M. 1983, ApJ 268, L99

Stacey, G.J. Genzel, R., Lugten, J.B., Poglitsch, A., Sternberg, A., & Townes, C.H. 1991, ApJ 373, 423

Stacey, G.J, Jaffe, D.T., Geis, N., Genzel, R., Harris, A.I., Poglitsch, A.,Stutzki, J., & Townes, C.H. 1993, ApJ 404, 219

de Vaucouleurs, G., Pence, W.D., & Davoust, E. 1983, ApJ S, 53, 17

Wolfire, M.G., Tielens, A.G.G.M., & Hollenbach, D. 1990, ApJ 358, 116